Generalized Predictive Speed Control of Two-Motor Drive Machines Series-Connected Fed by Five-Phase

Taieb Bessaad[1*], Khelifa Khelifi Otmane[2], Abderrahmen Benbouali[1], Rachid Taleb[1], Ali Bouchaib[1], Iqbel Atif[3]

[1]Electrical Engineering Department, Hassiba Benbouali University of Chlef, Laboratoire Génie Electrique et Energies Renouvelables (LGEER), Chlef, Algeria
t.bessaad@univ-chlef.dz, a.benbouali@univ-chlef.dz, r.taleb@univ-chlef.dz, a.bouchaib@univ-chlef.dz

[2]Automatic and Electrotechnical Department, Saad Dahlab University - Blida 1, Blida, Algeria
khelifi_khelifa@univ-blida.dz

[3]Electrical Engineering Department, Qatar University, Qatar
atif.iqbal@qu.edu.qa

Abstract: This work examines a newly introduced five-phase drive system with two motors and stator windings connected in series. Using a widely recognized phase transposition in the series chain, it is shown how a single five-phase SVPWM inverter can power a two series-connected five-phase machine drive with decoupled torque and flux control.

The exceeded generated current is among the many important problems: quick, with significant change in step of the speed control of a single inverter-supplied both 5-phase synchronous drive machines connected in series. Consequently, if the speed controller lacks output amplitude limitation, it may cause damage to the motor itself as well as the power electronics converter. This study's goal is to solve saturating speed controller issue. First, a speed control loops and both internal current loops are the two applications for controllers that are predictive in polynomial form.

*In order to make sure that the reference speed response stays within an enforced template under temporary conditions with a low current command, the outer predictive controller for speed is then enhanced by optimizing the Youla parameter convexly while taking frequency and temporal constraints into account. On the other hand, the new controller maintains the closed loop's properties that the original predicting controller. The results of the simulation confirm the validity and effectiveness of the control strategy proposed **G**eneralized **P**redictive **C**ontrol GPC_RST of the multi-machines system in both terms of performance and robustness (the stator resistance $R_{s1,2}$ and the inertia variation $J_{1,2}$ have been doubled, and the inductances $L_{d1,2}$ and $L_{q1,2}$ have been lowered by 20% of their nominal values) compared to the conventional **P**roportional **I**ntegral PI controllers.*

Keywords: multi-machines; 5-phase inverter; Vector control; predictive control

1 Introduction

Numerous studies on multi-phase motors which are better than three-phase have been published in the literature. When compared to three-phase machines, they have been shown to have a number of advantages, such as low ripple current [1], stability and fault tolerance [2], high torque density [3], [4], and decreased torque pulsations [5], [6]. As a result, machines with many phases of order are often evaluated to feed certain application domains such as electric airplanes, ship propulsion, robots, and electric/hybrid vehicles. In [7], and [8], comprehensive evaluations of the study and It is proposed that multi-phase machines be developed.

The parallel and/or series connections of multi-phase machines are among their uses. This type of drive system is called as a two-motor drive system that is coupled in series and parallel. This driving system is powered by a variable frequency and variable voltage source, often a power electronic inverter. It was initially presented in [9], [10].

What the driving system is set up so that machines may run at different speeds and carry varying weights without interfering with one another.

Additionally, the drive topology does not specify the kind of machines used [11]. The vector control method is used to operate the machines.

Since vector controllers for multi-phase motors require both stator current components, to control more motors, an additional stator current component is used. [12]. Therefore, It will be possible to function separately each motor that displays the supply as a separate multiple phases of source voltage inverter by constructing a connection in series for stator windings with many phases [13]. This idea is most evident in the parallel/serie-connected a chain with five phase two-motor drives, which consists of both five phase motors and is fed by a single VSI with five phases. A thorough analysis of this topology may be found in [14], [15].

Several methods, including predictive tactics, are available for controlling the speed of a five-level inverter-supplied, series-connected, five-phase drive. Numerous research labs have developed and have been interested in predictive control applications for electric drives [16-21] and [22]. Furthermore, To control many electric motor loops, the researchers of [23] and [24] employ the cascaded generalized predictive control (GPC) [25-30] method; other writers used the multivariable GPC formulation to regulate various system variables [16]. A single five-phase inverter supplies a Machine drives (M1) and (M2) with five phases that is coupled in series with a vector-controlled system is created by cascading two feedback loops.

A current regulation loop makes up the inner loop, whilst the outer loop regulates speed. The studies that when used to govern two synchrnous motors, the GPC control technique with RST polynomial structure produced remarkably robust results, optimality, and capacity to confront uncertainty when compared to the traditional PI controllers.

The aforementioned electrical drive has limitations, including maximum permitted motor current and power inverter constraints, which make it a challenging technical challenge in practice, particularly when it comes to high speed control. The GPC speed controller can produce an exceeding q, y-axis currents reference for the GPC currents controller in dynamic and high-speed profiles if it is constructed in a linear area without taking into account any constraints. This can result in an overmodulation in the inverter. Additionally, in practice, this current command is restricted to a specified maximum value that is dependent on the magnetic saturation, excessive stator winding heat, and a limit of the inverter's maximum current.

A lengthy time of settling, a significant exceed on the response of speed, and regardless he instability of the system result from the so-called windup phenomena, which occurs when the GPC speed controller is saturated and the close-loop performance deteriorates in comparison to the predicted linear performance. Therefore, the management of the two motors requires the employment of sophisticated control that respects these limitations while maintaining a basic structural design in order to protect the system's two motors and power electronics.

By using the Youla parametrization, this study aims to implement a straightforward and efficient method to avoid the GPC speed controller saturation. A unified off-line technique for retuning an initial GPC law while maintaining its two degrees of freedom form is presented by the authors in [31-33] using the Youla parametrization. Convex optimization is used to complete tracking behavior and closed loop features in terms of two free parameters, Q_1 and Q_2, in this parametrization are separated. Consequently, the Q_2 has no effect on the closed loop performances and can only alter the input output transfer functionIn order to prevent controller saturation and preserve the GPC characteristics, we shall utilize this feature on our electrical drive in this study.

Using the load torque and speed reference, the estimate and control scheme's performance is evaluated. Despite being connected in series and powered by a single inverter. These results show that under severe load and speed variations, the two machines are totally disconnected. Furthermore, an analysis is presented that compares GPC to the conventional PI for sensorless operation.

The purpose of this paper is to investigate control (GPC) for series-connected two-motors powered by a single five inverter. To obtain the desired characteristics, the GPC controllers are implemented for speeds and currents to increase its robustness (parameters variations of the two machines). In addition, an exact decoupling between the speed and the flux is realized by this strategy in wide speed ranges and makes it possible to obtain the best performances in the presence of disturbances. The developed control scheme combines the features of robust control and the robust estimation to enhance the performances of the proposed two-machine drives.

Moreover, a comparison between the conventional regulator PI and GPC controller operation is also provided.

The paper is structured as follows. Section 2 presents the mathematical modeling of the two series-connected five-phase PMSMs and outlines the key assumptions used in the analysis. Section 3 introduces the design of the Generalized Predictive Control (GPC) strategy tailored for the system under consideration. In Section 4, the implementation details of the proposed control scheme are discussed, including its integration with the single five-phase inverter. Section 5 provides simulation and experimental results to validate the performance of the proposed method. Finally, Section 6 concludes the paper with a summary of findings and potential directions for future work.

2 Model of the Multi-Machine System Connected in Series

Two five-phase PMSMs coupled in series consist the multi-machine system (Fig. 1). A single five-phase power source powers the two motors, five-phase inverter. The angle of the spatial phase shift between two successive phase stators is 72° for each machine in the system.

In Figure 1, the two machines in the system are assumed to have the same parameters and the electrical circuit of the model can be written as follows:

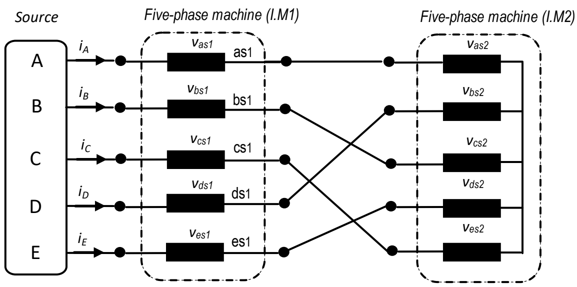

Figure 1
Diagram of coupling the phase windings in series of the stator of the multi-motors. A five-phase inverter powers the system

The following is the state space form of the phase variable model of system multi-machines (PMSM) connected in series as shown in Figure 1:

$$\left[V_{ABCDEF}\right]=\left[R_S\right]\left[i_{ABCDE}\right]+\frac{d}{dt}\left[\varphi_{ABCDEF}\right] \tag{1}$$

Figure 1 shows the link between each machine's stator currents and source currents, as well as the stator voltages of two five-phase machines connected in series and the inverter voltages (A, B, C, D, E, and N).

$$\left[V_s\right]=\begin{bmatrix} v_A \\ v_B \\ v_C \\ v_D \\ v_E \end{bmatrix}=\begin{bmatrix} v_{as1}+v_{as2} \\ v_{bs1}+v_{cs2} \\ v_{cs1}+v_{es2} \\ v_{ds1}+v_{bs2} \\ v_{es1}+v_{ds2} \end{bmatrix} \tag{2}$$

The following are the stator voltages of two five-phase machines linked in series, (A, B, C, D, E, and N) are the converter's voltages, and the connection between each machine's source and stator currents as shown in Fig. 1:

$$\left[i_s\right]=\begin{bmatrix} i_A \\ i_B \\ i_C \\ i_D \\ i_E \end{bmatrix}=\begin{bmatrix} i_{as1} \\ i_{bs1} \\ i_{cs1} \\ i_{ds1} \\ i_{es1} \end{bmatrix}=\begin{bmatrix} i_{as2} \\ i_{cs2} \\ i_{es2} \\ i_{bs2} \\ i_{ds2} \end{bmatrix} \tag{3}$$

The power-invariant Clark's decoupling transformation matrix is represented by relation (4):

$$\left[C\right]^t=\sqrt{\frac{2}{5}}\begin{bmatrix} 1 & cos(\alpha) & cos(2\alpha) & cos(3\alpha) & cos(4\alpha) \\ 0 & sin(\alpha) & sin(2\alpha) & sin(3\alpha) & sin(4\alpha) \\ 1 & cos(2\alpha) & cos(4\alpha) & cos(6\alpha) & cos(8\alpha) \\ 0 & sin(2\alpha) & sin(4\alpha) & sin(6\alpha) & sin(8\alpha) \\ 1/\sqrt{2} & 1/\sqrt{2} & 1/\sqrt{2} & 1/\sqrt{2} & 1/\sqrt{2} \end{bmatrix} \tag{4}$$

Moving to the new variables system (α,β,x,y,o) from the original system ($ABCDE$) as:

$f(\alpha\beta xy)=[C]f(ABCDE)$

With [C] is the power-invariant transformation matrix.

The voltages and currents of the five-phase inverter (α,β) and (x,y) are defined as:

$$\begin{bmatrix} v_\alpha^{inv} \\ v_\beta^{inv} \\ v_x^{inv} \\ v_y^{inv} \\ v_o^{inv} \end{bmatrix} = [C].\begin{bmatrix} v_A \\ v_B \\ v_C \\ v_D \\ v_E \end{bmatrix} = [C].\begin{bmatrix} v_{as1}+v_{as2} \\ v_{bs1}+v_{cs2} \\ v_{cs1}+v_{es2} \\ v_{ds1}+v_{bs2} \\ v_{es1}+v_{ds2} \end{bmatrix} = \begin{bmatrix} v_{\alpha s1}+v_{xs2} \\ v_{\beta s1}+v_{ys2} \\ v_{xs1}+v_{\alpha s2} \\ v_{ys1}+v_{\beta s2} \\ 0 \end{bmatrix} \tag{5}$$

$$\begin{cases} i_\alpha^{inv} = i_{\alpha s1} = i_{xs2} \\ i_\beta^{inv} = i_{\beta s1} = -i_{ys2} \\ i_x^{inv} = i_{xs1} = i_{\alpha s2} \\ i_y^{inv} = i_{ys1} = i_{\beta s2} \end{cases} \tag{6}$$

Since the two subs-paces (α,β) and (x, y) are orthogonal, as shown in Figure 1, the particular technique for connecting the system's two machines in series will enable the two machines to have independent vector control.

The zero-order component for the converter can also be well neglected. Eight first order equations represent the electromagnetic part of the drive system.

In (7), the four inverter/stator voltage equations are represented:

$$\begin{cases} v_\alpha^{inv} = (R_{s1}+R_{s2})i_\alpha^{inv} + (L_{sl1}+\frac{5}{2}m_{s1})\frac{d}{dt}i_\alpha^{inv} \\ \quad + L_{sl2}\frac{d}{dt}i_\alpha^{inv} - \sqrt{\frac{5}{2}}\Omega_1\phi_{f1}\,sin(\theta_1) \\ v_\beta^{inv} = (R_{s1}+R_{s2})i_\beta^{inv} + (L_{sl1}+\frac{5}{2}m_{s1})\frac{d}{dt}i_\beta^{inv} \\ \quad + L_{sl2}\frac{d}{dt}i_\beta^{inv} + \sqrt{\frac{5}{2}}\Omega_1\phi_{f1}\,cos(\theta_1) \end{cases} \tag{7}$$

$$\begin{cases} v_x^{inv} = (R_{s1}+R_{s2})i_x^{inv} + (L_{sl2}+\frac{5}{2}m_{s2})\frac{d}{dt}i_x^{inv} \\ \quad + L_{sl1}\frac{d}{dt}i_x^{inv} - \sqrt{\frac{5}{2}}\Omega_2\phi_{f2}\,sin(\theta_2) \\ v_y^{inv} = (R_{s1}+R_{s2})i_y^{inv} + (L_{sl2}+\frac{5}{2}m_{s2})\frac{d}{dt}i_y^{inv} \\ \quad + L_{sl1}\frac{d}{dt}i_y^{inv} + \sqrt{\frac{5}{2}}\Omega_2\phi_{f2}\,cos(\theta_2) \end{cases} \tag{8}$$

To represent every size in a single frame, the stator variables are projected onto a reference frame (*d, q*) that rotates and is displaced by φ in relation to the fixed coordinate system (α,β), this transformation is calculated from the matrix [D] rotation as:

$$\left[D\right]=\begin{bmatrix} cos(\theta) & sin(\theta) & . \\ sin(\theta) & cos(\theta) & . \\ . & . & \left[I\right]^{3\times 3} \end{bmatrix} \tag{9}$$

The two machines linked in series have the following torque equations:

$$\begin{cases} T_{e1}=p_1((L_d-L_q)i_d^{inv}.i_q^{inv}+\sqrt{\dfrac{5}{2}\phi_{f1}}.i_q^{inv}) \\ T_{e2}=p_2((L_x-L_y)i_x^{inv}.i_y^{inv}+\sqrt{\dfrac{5}{2}\phi_{f2}}.i_y^{inv}) \end{cases} \tag{10}$$

Using these equations and (6), it is evident that the first motor's torque currents (i_{sd}, i_{sq}) are zero, which results in the second motor's torque currents (i_{sx}, i_{sy}). A single VSI may therefore be used to independently regulate the two motors.

3 Two Five-Phase PMSMs Connected in Series for Independent Control

According to the (10), the first machine torque is controlled by the two currents (i_{sd}, i_{sq}) and for the second machine torque controlled by both current (i_{sx}, i_{sy}). Among the control strategies, Keeping the component i_{sd} and i_{sx} null is one that is frequently used. We control torques only by i_{sq} and i_{sy}.

For the machine 1

$$\begin{cases} v_d^{inv}=(R_{s1}+R_{s2})i_d^{inv}+(L_{sl1}+\dfrac{5}{2}m_{s1})\dfrac{d}{dt}i_d^{inv} \\ \qquad +L_{sl2}\dfrac{d}{dt}i_d^{inv}-\Omega_1(L_{sl1}+\dfrac{5}{2}m_{s1})i_q^{inv} \\ v_q^{inv}=(R_{s1}+R_{s2})i_q^{inv}+(L_{sl1}+\dfrac{5}{2}m_{s1})\dfrac{d}{dt}i_q^{inv} \\ \qquad +L_{sl2}\dfrac{d}{dt}i_q^{inv}-\Omega_1(L_{sl1}+\dfrac{5}{2}m_{s1})i_d^{inv}+\sqrt{\dfrac{5}{2}}\Omega_1\phi_{f1} \end{cases} \tag{11}$$

For the machine 2

$$\begin{cases} v_x^{inv} = (R_{s1} + R_{s2}) i_x^{inv} + (L_{sl1} + \frac{5}{2} m_{s2}) \frac{d}{dt} i_x^{inv} \\ \quad + L_{sl1} \frac{d}{dt} i_x^{inv} - \Omega_2 (L_{sl2} + \frac{5}{2} m_{s2}) i_y^{inv} \\ v_y^{inv} = (R_{s1} + R_{s2}) i_y^{inv} + (L_{sl1} + \frac{5}{2} m_{s2}) \frac{d}{dt} i_y^{inv} \\ \quad + L_{sl1} \frac{d}{dt} i_y^{inv} - \Omega_2 (L_{sl2} + \frac{5}{2} m_{s2}) i_x^{inv} + \sqrt{\frac{5}{2}} \Omega_2 \phi_{f2} \end{cases} \tag{12}$$

Figure 2's wiring schematic is then used to provide the overall voltage references, while [11]:

$$\begin{bmatrix} V_a^* \\ V_b^* \\ V_c^* \\ V_d^* \\ V_e^* \end{bmatrix} = \begin{bmatrix} v_{as1}^* + v_{as2}^* \\ v_{bs1}^* + v_{cs2}^* \\ v_{cs1}^* + v_{es2}^* \\ v_{ds1}^* + v_{bs2}^* \\ v_{es1}^* + v_{ds2}^* \end{bmatrix} \tag{13}$$

The transfer functions shown below represent the electric and mechanical modes, respectively:

$$\begin{cases} G_{ik}(S) = \dfrac{1}{(R_{ik} + \sigma_k L_{sk}.S)} \\ G_{sk}(S) = \dfrac{1}{(f_{rk} + J_k.S)} \end{cases} \tag{14}$$

Where k is the machine number (k=1: first machine M1, k=2: second machine M2).

Transfer functions (14) need to be transformed into discrete time transfer functions as the GPC controllers are discrete in nature.

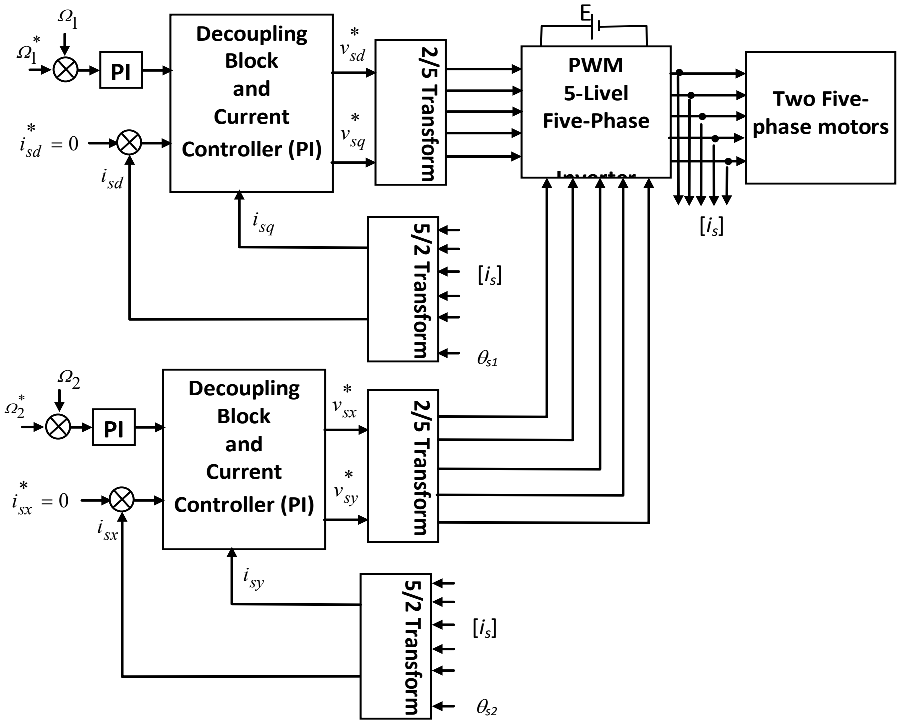

Figure 2

Vector control of currents and speeds of the Multi-imachines system fed by a five level inverter

Thus, the ZOH (zero order hold) discretization method may be used to produce the z-transform of the system transfer functions (14) as follows:

$$\begin{cases} G_{ik}(q^{-1}) = \dfrac{q^{-1}A_{ik}(q^{-1})}{B_{ik}(q^{-1})} \\ G_{sk}(q^{-1}) = \dfrac{q^{-1}A_{sk}(q^{-1})}{B_{sk}(q^{-1})} \end{cases} \tag{15}$$

The models utilized in the construction of the GPC controllers for speed and currents, respectively, are the transfer functions that were previously developed.

The block diagram of vector command scheme for a five-phase, two-motor drive system based on the FOC method is shown in Figure 2. When the two motors' speeds beyond their nominal values, the flux reference is guaranteed to decrease due to field weakening. Using the Park's transformation, the *ABCDEF =>d,q,x,y* block gets the $i_{as}, i_{bs}, i_{cs}, i_{ds}, i_{es}, i_{fs}$, motor stators currents and the *dq xy=>ABCDEF* block makes the reverse Park’s transformation

The $i_{as}, i_{bs}, i_{cs}, i_{ds}, i_{es}, i_{fs}$ and motor stator currents are obtained using the Park's transformation in the *ABCDEF => dqxy* block, and the reverse Park's transformation is made in the *dqxy => ABCDEF* block.

4 Standard Generalized Predictive Controller

The GPC control technique employs controlled autoregressive integrated moving average model (CARIMA) for prediction in both situations (speed loop and current loops):

$$A_k(q^{-1})y_k(t) = B_k(q^{-1})u_k(t) + \frac{\xi_k(t)}{\Delta(q^{-1})} \tag{16}$$

$y_k(t)$, $\xi_k(t)$: represent process output and zero mean white noise respectively, $\Delta(q^{-1}) = 1 - q^{-1}$, $u_k(t)$ is the control signal, and A_k and B_k are polynomials in backward shift operator q derived from (16).

The *j-th* prediction step's expected output across the costing horizons $N_{1k} \le j \le N_{2k}$ is determined by:

$$\begin{aligned} y_k(t+j) &= F_{jk}(q^{-1})y_k(t) + H_{jk}(q^{-1})\Delta u_k(t-1) \\ &\quad + G_{jk}(q^{-1})\Delta u_k(t+j-1) + J_{jk}(q^{-1})\xi_k(t+j) \end{aligned} \tag{17}$$

The cost function is minimized to provide the GPC control law Presented by: Polynomials Fj_k, Gj_k and Hj_k are found by repeatedly solving Diophantine equations.

To achieve optimal command values, the GPC uses a quadratic cost function defined as:

$$\begin{aligned} &J_k(N_{1k}, N_{2k}) = \sum_{j=N_{1k}}^{N_{2k}} \left[\hat{y}_k(t+j) - w_k(t+j)\right]^2 + \lambda_k \sum_{j=1}^{N_{uk}} \left[u_k(t+j-1)\right]^2 \\ &\Delta u_k(t+j) = 0 \quad for\ j \ge N_{uk} \end{aligned} \tag{18}$$

Where N_{uk} is the control horizon, N_{1k} and N_{2k} are the lowest and maximum costing horizons, w_k is the set-point, and λ_k : represents the element of control weighting.

$\hat{y}_k$ is the predicted output value, obtained solving Diophantine equation, and u_k is the control signal.

In our GPC design, the **optimization variables** are the future control increments $\Delta u_k(t)$, $\Delta u_k(t+1)$,….. $\Delta u_k(t+N_{uk}-1)$, where N_{uk} is the control horizon

These increments represent the change in control input (i.e., torque-producing current commands such as $i_{qs}{}^{*}$ and $i_{ys}{}^{*}$) at each time step. The GPC algorithm computes the optimal sequence of these increments to minimize the cost function defined in Equation (18), which combines predicted tracking errors and control effort penalties. This approach enables smooth and stable speed tracking while avoiding abrupt changes in current that may lead to overmodulation or system stress.

The two degrees of freedom $(RST)_k$ structure shown in Figure 3 may be created from the acquired GPC control rule as follows:

$$S_k(q^{-1})\Delta(q^{-1})u_k(t) = -R_k(q^{-1})y_k(t) + T_k(q)w_k(t) \tag{19}$$

Thus, three GPC-RST controllers will be synthesized: two for the inner current loops, indicated by GPC current, and one for the outer speed control loop, represented by GPC speed.

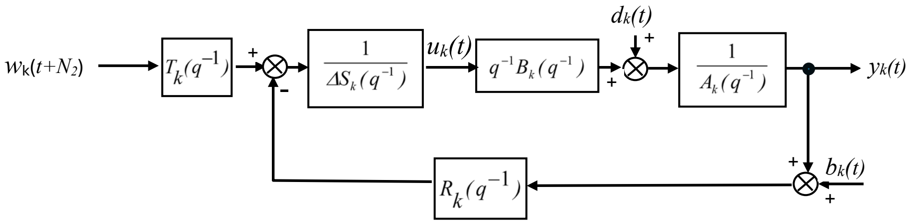

Figure 3

Polynomial RST controller comparable to GPC

Assuming that R_{0k}, S_{0k}, T_{0k}, and N_{1k}, N_{2k}, N_{uk}, and λ_k have been tweaked to meet certain closed loop performance requirements, the original GPC speed controller design has been completed. Since the GPC speed controller lacks an output magnitude limiter, as shown in Figure 2, the reference of the electromagnetic torque $T^*_{emu,k}$ can take on rather large values in transient regimes. As a result, the currents command i^*_{qs} and i^*_{ys}, particularly in high-speed profiles; hence, the significant control action may cause damage to the system drive.

This work's primary objective is to prevent current overflows without adding a limited to the output or sacrificing the close-loop performance that the original GPC speed controller achieved. Retuning the original controller using Youla parametrization will be the method used. The resultant controller needs to adhere to the specified boundaries.

5 Improved GPC Speed Controller

The initially released GPC speed controller as parameterized by Youla (R_{0k}, S_{0k},T_{0k}) yields the stabilizing polynomials shown below, in accordance with the work reported in [1]:

$$\begin{cases} T_k(q^{-1}) = T_{0k}(q^{-1}) - A_{0k}(q^{-1})Q_{2k}(q^{-1}) \\ R_k(q^{-1}) = R_{0k}(q^{-1}) - \Delta A_k(q^{-1})Q_{1k}(q^{-1}) \\ S_k(q^{-1}) = S_{0k}(q^{-1}) - q^{-1}B_k(q^{-1})Q_{1k}(q^{-1}) \end{cases} \tag{20}$$

where the transfer functions Q_{1k} and Q_{2k} are stable. Figure 4 displays the matching block diagram.

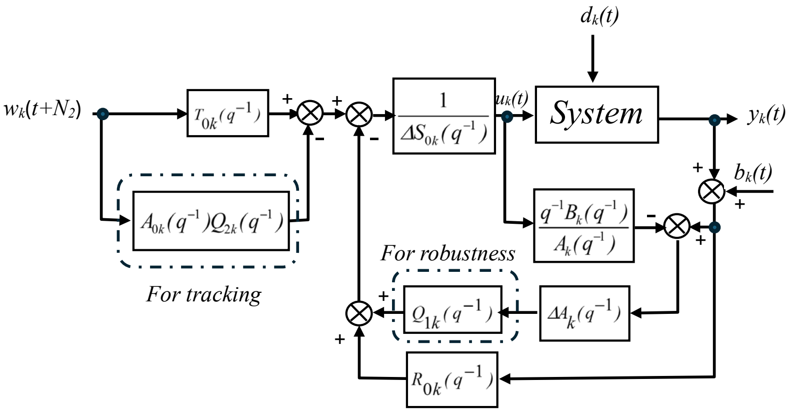

Figure 4

Youla parameterization for the GPC_RST controller

It may infer from Figure 4 that although the parameter Q_{2k} alters the closed loop characteristics while maintaining the input-output transfer, the parameter Q_{1k}

Only the input-output transfer function is altered. Since the initial controller design is sufficient to achieve closed loop performance, we set Q_{1k} to zero in the following. Q_{2k} will then be used to fine-tune this initial controller by altering the input-output behavior to avoid the undesirable high control signal at the GPC speed controller's output.

Time domain and frequency parameters are the two categories of standards that Q_{2k} is made to meet. In this case, the signals w_k, y_k , and u correspond receptively to the measured speedΩ_k, the speed reference (*), and the present commands i^*_{qs} and i^*_{ys}.

6 Discussions of Simulation Results

Using the Matlab / Simulink software, different the two series-connected machines in (MSCS) have their vector speed control simulation results generated.

Figures 5 and 6 illustrate how the both actuator series connected and fed by a five phase inverter may be independently controlled. The responses of the multi-machine system are achieved by a simulation.

To confirm that the both motors controls are independent different simulation tests are performed in order. The speeds, currents, and torques of the unloaded two are shown in Figures 5 and 6.

During the first test, the machine number one is operational at Ω=[200 to -200] rad/s at t=0.7 s and 2^{nd} machine was running at 150 rad/s, then -150rad/s at t=0.7 s of the reference speed.

The first and second machines applied load torques that were 100% of the speed reference's rated torque for the two machines at t = [0.2 – 0.4] s. Then, at =0.2 s and t=0.7 s load couples are applied to M1 and M2 respectively.

Figure 6 shows the simulation results of the second test, this test represented step change of the reference speed is represented, a step change of the reference speed from 200 rad/s to -200 rad/s at t=0.7 s for the first machine (M1) and -200 rad/s to 200 rad/s for second machine (M2) at t=0.7 s. At t = [0.2 – 0.4] s, load couples are applied to M1 and M2. From Figures 5 and 6, it can be noticed that the decoupled control is still retained, There has been no discernible impact on the two devices' characteristic has been observed.

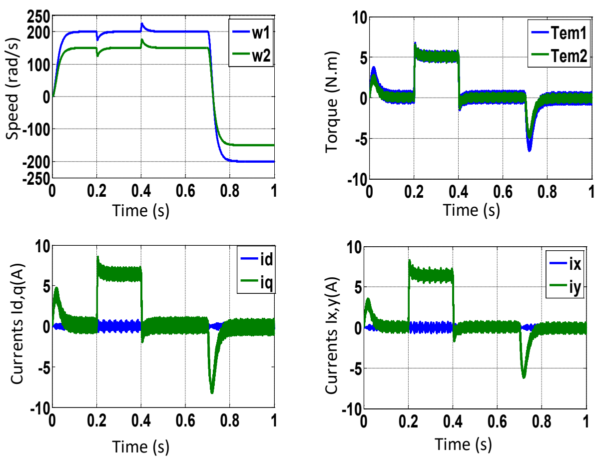

Figure 5

System PMSM's responses with a load of 5 Nm at [0.2-0.4] s and a step change of two speeds order(200 rad/s and 150 rad/s)

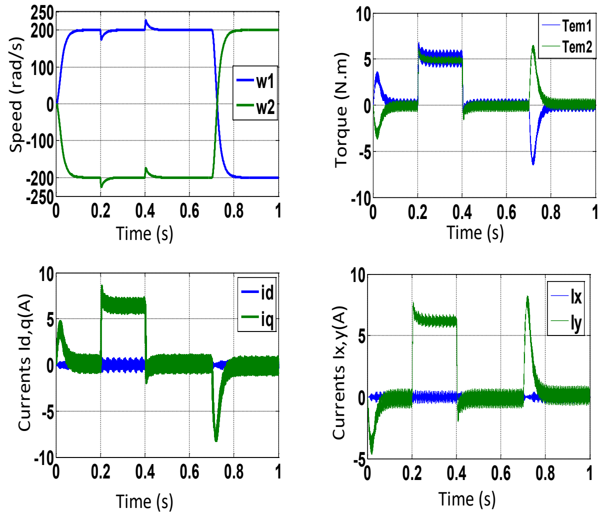

Figure 6
The PMSM's responses with a load of 5 Nm at [0.2-0.4] s and a step change of the reference speed for M1 and M2

7 Test of Robustness

The test to evaluate the impact of both machines of the sysytem (PMSM) parameter adjustment on how well the regulators operate is displayed in Figure 7. The motor is operating at its stated speed. The machine's parametres have been changed to test the durability of the controllers used: the stator resistance $R_{s1,2}$ and the inertia variation $J_{1,2}$ have been doubled, and the inductances $L_{d1,2}$ and $L_{q1,2}$ have been lowered by 20% of their nominal values.

Figure 7 displays the obtained results. These findings demonstrate that the five-phase PMSM's parameter changes affect the speed curves in a discernible way, and that the influence is greater for the classical regulator (PI) than for GPC control. We can infer from this result that these final controllers are more resilient.

(a)

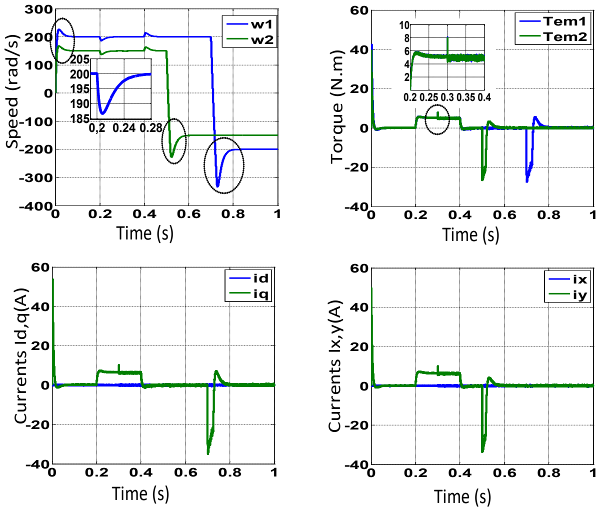

(FOC, PI controllers)

(b)

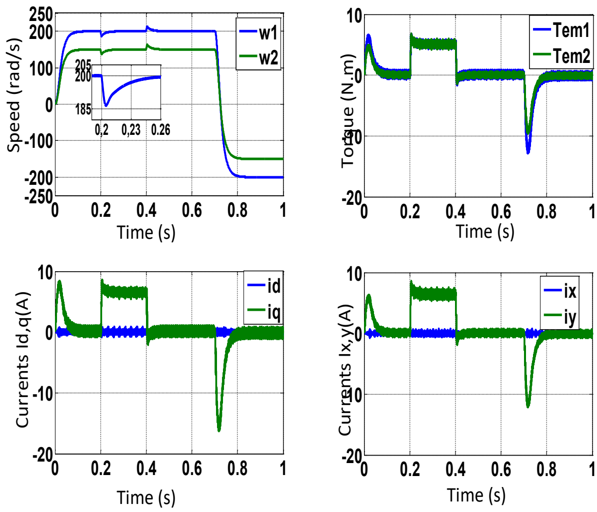

(GPC)

Figure 7

The PMSM's responses at Rs ,J and Ld Lq variations for M1 and M2

Conclusion

Using this method, we tested vector control in simulation on both 5-phase synchronous motors (M1 and M2) of the system that were fed by a single inverter connected in series.

We were able to order two machines separately by transposing them, which gave us greater flexibility on the existing axis.

With proper dynamics, the speeds and fluxes follow their references because throughout the transitory of the first machine speed, the flux of the second machine is unchanged, and vice versa; also, the speeds are nearly unaltered.

Comparing control with proposed controller to the traditional controllers, the results of the simulation confirm the validity and effectiveness of the control strategy proposed of the multi-machines system in both terms of performance and robustness (the stator resistance $R_{s1,2}$ and the inertia variation $J_{1,2}$ have been doubled, and the inductances $L_{d1,2}$ and $L_{q1,2}$ have been lowered by 20% of their nominal values.) compared to the conventional controllers.

Table 1

Machines Parametres

R_s	L_d	L_q	J	p	flux
3.6 ohm	0.0021 H	0.0021 H	0.0011kg/m²	2	0.25 web

References

[1] W. Ben Mabrouk, J. Belhadj, M. Pietrzak-David: Modelling and Control of electromechanical Multi-machine System for Railway Traction, 2nd International conference on Electrical Engineering Design and Technologies, ICEEDT, 8-10, Hammamet Tunisia, 2008

[2] E. Levi, M. Jones, S. N. Vukosavic, A. Iqbal, and H. A. Toliyat: Modeling, control, and experimental investigation of a five-phase series-connected two-motor drive with single inverter supply, IEEE Trans. Ind. Electron. Jun, 2007

[3] E. Levi, M. Jones, S. N. Vukosavic, H. A. Toliyat: A novel concept of a multi-phase, multi-motor vector controlled drive system supplied from a single voltage source inverter, IEEE Transactions on Power Electronics, Vol. 19, No. 2, pp. 320-335, 2004

[4] D. Dujic, G. Grandi, M. Jones, and E. Levi: A space vector PWM scheme for multifrequency output voltage generation with multiphase voltage-source inverters, IEEE Transactions on Industrial Electronics, Vol. 55, No. 5, pp. 1943-1955, May 2008

[5] J. Staszak, K. Ludwnek, Z. Gawecki, J. Kurkiewicz and T. Bekier: Utilization of Permanent Magnet Synchronous Motors in Industrial Robot,

IEEE International Conference on Information and Digital Technologies, Zilina, Slovakia, pp. 342-347, 2015

[6] R. Peña-Eguiluz, M. Pietrzak-David, B. de Fornel: Enhanced locomotive drive system behaviour applying a single voltage source inverter dual induction motor structure, EPE Journal, Vol. 15, No. 2, 2005

[7] E. Semail, E. Levi, A. Bouscayrol, X. Kestelyn: Multi-Machine Modelling of Two Series Connected 5-phase Synchronous Machines: Effect of Harmonics on Control, IEEE-IAS'04, Seattle (Washington), October 2004

[8] M. J. Duran, F. Salas, and M. R. Arahal: Bifurcation analysis of five-phase induction motor drives with third harmonic injection, IEEE Transactions on Industrial Electronics, Vol. 55, No. 5, pp. 2006-2014, May 2008

[10] N. Lavanya and M. Venu Gopala Rao: Control of Indirect Matrix Converter by Using Improved SVM Method, International Journal of Power Electronics and Drive System (IJPEDS), Vol. 6, No. 2, pp. 370-375, 2015

[11] D. Sri Vidhya, T. Venkatesan: A Review on Performance Analysis of Matrix Converter Fed AC Motor Drive, International Journal of Power Electronics and Drive System (IJPEDS), Vol. 7, No. 1, pp. 85-93, 2016

[12] E. Levi: Multiphase Electric Machines for Variable-Speed Applications, in IEEE Transactions on Industrial Electronics, Vol. 55, No. 5, pp. 1893-1909, 2008

[13] M. Jones, E. Levi and S. N. Vukosavic: Independent Control of Two Five-Phase Induction Machines Connected in Parallel to a Single Inverter Supply, IECON 2006 - 32nd Annual Conference on IEEE Industrial Electronics, pp. 1257-1262, 2006

[14] E. Levi, A. Iqbal, S. N. Vukosavic and H. A. Toliyat: Modeling and control of a five-phase series-connected twomotor drive, IECON'03. 29th Annual Conference of the IEEE Industrial Electronics Society (IEEE Cat. No.03CH37468), Vol. 1, pp. 208-213, 2003

[15] E. Levi, M. Jones, S. N. Vukosavic, H. A. Toliyat: A five-phase twomachine vector controlled induction motor drive supplied from a single inverter, European Power Electronics and Drives, Vol. 14, No. 3, pp. 38-48, 2004

[16] H. Wang, W. Zhao, H. Tang, T. Tao, and S. Saeed: Improved fault-tolerant model predictive torque control of five-phase PMSM by using deadbeat solution, IEEE Transactions on Energy Conversion, Vol. 37, No. 1, pp. 210-219, 2022

[17] D. Zhao, N. Zhao, H. Zhang, P. Shi, I. Rudas: Resilient Sampled-Data Event-Triggered Control for Switched Systems Under Denial of Service Attacks, Acta Polytechnica Hungarica Vol. 21, No. 10, 2024

[18] R. C. Roman, R. Precup, E M. Petriu: Active Disturbance Rejection Control for 3D Crane Systems, Procedia Computer Science, Vol. 242, No. 4, pp. 976-983, 2024

[19] I. A. Zamfirache, R. E. Precup, E. M. Petriu: Adaptive reinforcement learning-based control using proximal policy optimization and slime mould algorithm with experimental tower crane system validation, Applied Soft Computing, Vol. 160, No. 1, pp. 111687, 2024

[20] T. Haidegger, L. Kovács, R. E. Precup, B. Benyó, Z. Benyó, S. Preitl: Simulation and control for telerobots in space medicine, Acta Astronautica, Vol. 81, No. 1, pp. 390-402, 2012

[21] Á. Takács, L. Kovács, I. J. Rudas, R. E. Precup, T. Haidegger: Models for force control in telesurgical robot systems, Acta Polytechnica Hungarica,Vol. 12, No. 8, pp. 95-114, 2015

[22] R. C. Roman, R. E. Precup, E. M. Petriu, and A. Ioana. Borlea: Hybrid Data-Driven Active Disturbance Rejection Sliding Mode Control with Tower Crane Systems Validation, Romanian Journal of Information Science and Technology, Vol. 27, No. 1, pp. 50-64, 2024

[23] W. Huang, W. Hua, and Q. Fan: Performance analysis and comparison of two fault-tolerant model predictive control methods for five-phase PMSM drives, CES Transactions on Electrical Machines and Systems,Vol. 5, No. 4, pp. 311-320, 2021

[24] J. Beerten, J. Verveckken, J. Driesen: Predictive direct torque control for flux and torque ripple reduction, IEEE Trans. Ind. Electron. Vol. 57, No. 1, pp. 404-412, 2010

[25] H. Lu, J. Li, R. Qu, D. Ye, and L. Xiao: Reduction of unbalanced axial magnetic force in postfault operation of a novel six-phase double-stator axial-flux PM machine using model predictive control, IEEE Transactions on Industry Applications, Vol. 53, No. 6, pp. 5461-5469, 2017

[26] H. Guzman, M. J. Duran, F. Barrero, B. Bogado, and S. Toral: Speed control of five-phase induction motors with integrated open-phase fault operation using model-based predictive current control techniques, IEEE Transactions on Industrial Electronics, Vol. 61, No. 9, pp. 4474-4484, 2014

[27] W. Huang, W. Hua, F. Chen, and J. Zhu: Enhanced model predictive torque control of fault-tolerant five-phase permanent magnet synchronous motor with harmonic restraint and voltage preselection, IEEE Transactions on Industrial Electronics, Vol. 67, No. 7, pp. 6259-6269, 2020

[28] T. Tao, W. Zhao, Y. Du, Y. Cheng, and J. Zhu: Simplified fault-tolerant model predictive control for a five-phase permanent-magnet motor with reduced computation burden, IEEE Transactions on Power Electronics, Vol. 35, No. 4, pp. 3850-3858, 2020

[29] P. Alkorta, O. Barambones, A. J. Garrido, I. Garrido: SVPWM linear generalized predictive control of induction motor drives, In: Proceedings of the IEEE International Symposium on Industrial Electronics (ISIE ’08) Cambridge, UK, pp. 588-593, 2008

[30] A. Oshin, H. Almubarak, and E. A. Theodorou: Differentiable robust model predictive control, arXiv preprint, arXiv:2308.08426, 2023

[31] A. Romero, E. Aljalbout, Y. Song, and D. Scaramuzza: Actor-critic model predictive control: Differentiable optimization meets reinforcement learning, arXiv preprint, arXiv:2306.09852, 2023

[32] H. Wang, W. Zhao, H. Tang, T. Tao, and S. Saeed: An improved model-free current predictive control of permanent magnet synchronous motor based on high-gain disturbance observer, IEEE Transactions on Energy Conversion, Vol. 37, No. 1, pp. 210-219, 2022

[33] Z. Xue, S. Niu, and A. Man: Recent advances in multi-phase electric drives model predictive control in renewable energy application: A state-of-the-art review, Energies, Vol.b14, No. 2, pp. 44, 2022

[34] H. Cao, M. Cheng, and Y. Zhao: Robust three-voltage-vector-based model-free predictive current control strategy for PMSM drives, IET Power Electronics, Vol. 16, No. 5, pp. 834-843, 2023

[35] J. Rodriguez, A. Munoz, F. Barrero, and M. Jones: Model predictive control for multiphase motor drives – A technology status review, IEEE Transactions on Industrial Electronics, Vol. 63, No. 2, pp. 428-437, 2018

[36] A. Benmiloud, L. Saidi, and M. A. Djemai: Generalized predictive control of multi-phase induction machine supplied by multi-level inverter, Engineering, Physics & Sciences Teaching and Educational Methodology (EPSTEM), Vol. 10, No. 1, pp. 52-60, 2024